New approach to investigate nonlinear dynamic response of sandwich auxetic double curves shallow shells using TSDT

Pham Hong Cong[a,b], Nguyen Duy Khanh[a], Nguyen Dinh Khoa[a], Nguyen Dinh Duc[a,c,d,*]

[a] Advanced Materials and Structures Laboratory, VNU-Hanoi, University of Engineering and Technology (UET), 144 Xuan Thuy, Cau Giay, Hanoi, Viet Nam
[b] Centre for Informatics and Computing (CIC), Vietnam Academy of Science and Technology, 18 Hoang Quoc Viet, Cau Giay, Hanoi, Viet Nam
[c] Infrastructure Engineering Program, VNU-Hanoi, Vietnam-Japan University (VJU), My Dinh 1, Tu Liem, Hanoi, Viet Nam
[d] National Research Laboratory, Department of Civil and Environmental Engineering, Sejong University, 209 Neungdong-ro, Gwangjin-gu, Seoul 05006, Republic of Korea

ARTICLE INFO

ABSTRACT

Nonlinear dynamic behavior of double curved shallow shells with negative Poisson's ratios in auxetic honeycombs on elastic foundations subjected blast, mechanical and damping loads is investigated in the present article. This study considers double curved shallow shells with auxetic core which have three layers in which the top and the bottom outer skins are isotropic aluminum materials; the central layer has honeycomb structure using the same aluminum material. Based on the analytical solution, Reddy's third order shear deformation theory (TSDT) with the geometrical nonlinear in von Karman and Airy stress functions method, Galerkin method and the fourth-order Runge-Kutta method, the resulting equations are solved to obtain expressions for nonlinear motion equations. The effects of geometrical parameters, material properties, elastic foundations, imperfections, blast loads, mechanical and damping loads on the nonlinear dynamic analysis of double curved shallow shells with negative Poisson's ratios in auxetic honeycombs are studied.

1. Introduction

The composite auxetic material with negative Poison's ratio is a new material which has many outstanding benefits such as: lightweight, high durability and energy absorption capacity from loads, especially under blast load. For example, an application of lightweight auxetic composite plate to enhance the ballistic and impact resistance capabilities of armoured vehicles (Fig. 1) [1].

Therefore, the composite auxetic material with negative Poisson's ratio has been applied in so many important sectors for civil and defense purposes. Therefore, there have many studies on composite auxetic material with negative Poisson's ratio. Whitty et al. [2] studied towards the design of sandwich panel composites with enhanced mechanical and thermal properties by variation of the in-plane Poisson's ratios. Massimo Ruzzene et al. [3] studied the wave propagation in sandwich plates with periodic auxetic core. Qing-Tian and Zhi-Chun [4] investigated the wave propagation in sandwich panel with auxetic core. Qiao and Chen [5] considered impact resistance of uniform and functionally graded auxetic double arrowhead honeycombs. Miller et al. [6] investigated the negative Poisson's ratio carbon fibre composite using a negative Poisson's ratio yarn reinforcement. A number of numerical methods have been used to study the dynamic response of auxetic plate

and shell such as: Zhang et al. [7] considered the dynamic thermomechanical and impact properties of helical auxetic yarns. Strek et al. [8] considered the dynamic response of sandwich panels with auxetic cores. Ghaznavi and Shariya [9] studied the non-linear layerwise dynamic response analysis of sandwich plates with soft auxetic cores and embedded SMA wires experiencing cyclic loadings. Xiaochao Jin et al. [10] investigated the dynamic response of sandwich structures with graded auxetic honeycomb cores under blast loading. Sofiyev et al. [11] investigated the stability and vibration of sandwich cylindrical shells containing a functionally graded material core with transverse shear stresses and rotary inertia effects. Li et al. [12] considered the Dynamic behavior of aluminum honeycomb sandwich panels under air blast. Using analytical methods to study vibration and dynamic response of plate and shell with negative Poisson's ratios was applied by Duc et al. [13–15]. In [13–15], the authors considered vibration and dynamic response of the plate [13], panel [14] and double curved shallow shells [15] with negative Poisson's ratios in auxetic honeycombs layer on elastic foundations subjected to blast and damping loads using analytical solution, but they used the first order shear deformation theory.

In recent years, the safety of buildings and structures of infrastructure have become hot issues in all over the world because the negative dynamic loads caused of increasing in terrorist activities,

---

accidental blast. Nelson Lam et al. [16] studied the response spectrum solutions for blast loading. Lu et al. [17] considered the buried structure in soil subjected to blast load using 2D and 3D numerical simulations. [18] investigated the nonlinear structural response of laminated composite plates subjected to blast loading. [19] examined the nonlinear dynamic response and vibration of imperfect shear deformable functionally graded plates subjected to blast and thermal loads. Gabriele Imbalzano et al. [20,21] considered blast resistance of auxetic and honeycomb sandwich panels: Comparisons and parametric designs [20] and numerical study of auxetic composite panels under blast loadings [21].

Applying analytic method, stress function and Galerkin method to study dynamic response of FGM plate and shell structures using Reddy's third order shear deformation theory were mentioned in [22–25]; in which [23] studied plate, [24] about circular cylindrical shells, [25] about double curved thin shallow shells.

Recently, nanocomposite and CNT-reinforced composite have gradually gained interestes: Reza Kolahchi et al. [26] considered visco-nonlocal-refined Zigzag theories for dynamic buckling of laminated nanoplates using differential cubature-Bolotin methods. Maryam Shokravi [27] considered dynamic pull-in and pull-out analysis of viscoelastic nanoplates under electrostatic and Casimir forces via sinusoidal shear deformation theory. Reza Kolahchi et al. [28] studied the dynamic stability analysis of temperature-dependent functionally graded CNT-reinforced visco-plates resting on orthotropic elastomeric medium. Hamid Madani et al. [29] examined the differential cubature method for vibration analysis of embedded FG-CNT-reinforced piezoelectric cylindrical shells subjected to uniform and non-uniform temperature distributions. Reza Kolahchi et al. [30] investigated wave propagation of embedded viscoelastic FG-CNT-reinforced sandwich plates integrated with sensor and actuator based on refined zigzag theory.

From the above literature review, it can be seen that some research used numerical methods (finite element method) to study the dynamic of sandwich plate and shell with auxetic (without both elastic foundations and under blast load) [7–12]. The nonlinear dynamic response of the auxetic material under blast load on elastic foundations using analytical methods (approximately experimental form, stress function method) and the first order shear deformation theory was considered in [13–15]. Ref. [14] investigated dynamic response of the sandwich double curves shallow shells with auxetic honeycombs (the third order shear deformation theory has not been used yet).

Using Reddy's third order shear deformation theory (TSDT), accounting for both the von - Karman nonlinearity and analytical solution to study the dynamic response of the double curved shallow shells with negative Poisson's ratios in auxetic honeycombs layer on elastic foundations subjected to blast, mechanical and damping loads is investigated in the present work. The double curved shallow shells used in the paper have three layers in which the top and bottom outer skins are isotropic aluminum materials; the central layer has honeycomb structure using the same aluminum material. The work also analyses and discusses the effects of material and geometrical properties, elastic foundations, mechanical, imperfections, blast, mechanical and damping

loads on the nonlinear dynamic response of the double curved shallow shells with negative Poisson's ratios in auxetic honeycombs.

2. Sandwich double curves shallow shells with auxetic core

2.1. Model

As Fig. 1 shows, radius of curvature, length of edges and total thickness of the double curves shallow shells with auxetic core pate are denoted by R_x, R_y, a, b and $h = h_1 + h_2 + h_3$, respectively, where h_1, h_2 and h_3 are thickness of the top face sheet, core, and bottom face sheet, respectively. A coordinate system (x,y,z) is established, in which the (x,y) plane is in the middle surface of the panel and z is in the thickness direction (Fig. 2a). The auxetic core which has three layers in which the top and bottom outer skins are isotropic aluminum materials; the central layer has honeycomb structure using the same aluminum material (Fig. 2b).

The reaction–deflection relation of Pasternak foundation is given by

$$q_e = k_1 w - k_2 \nabla^2 w \tag{1}$$

in which $\nabla^2 = \frac{\partial^2}{\partial x^2} + \frac{\partial^2}{\partial y^2}$, w is the deflection of the double curves shallow shells, k_1 and k_2 are Winkler foundation modulus and shear layer of Pasternak foundation, respectively.

2.2. Honeycomb core materials

The double curves shallow shells with the auxetic honeycomb core with negative Poisson's ratio are introduced in this paper. Unit cells of core material discussed in the paper are shown in Fig. 3 where l is the length of the inclined cell rib, h is the length of the vertical cell rib, θ is the inclined angle, α and β define the relative cell wall length and the wall's slenderness ratio, respectively, which are important parameters in honeycomb property.

Formulas in Ref. [4] are adopted for calculation of honeycomb core material property
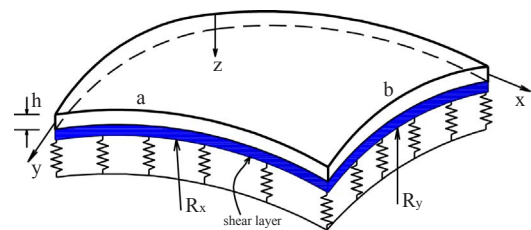
Fig. 2a. Model of sandwich double curves shallow shells with negative Poisson's ratios in auxetic honeycombs on elastic foundations.
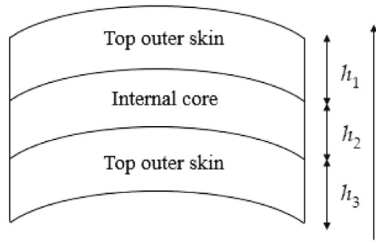
Fig. 2b. Discretization of the double curves shallow shells.
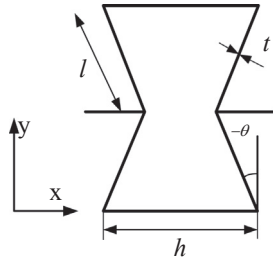
Fig. 3. Geometric of the cell of honeycomb core.

$$E_1^c = E\left(\frac{t}{l}\right)^3 \frac{\cos\theta}{\left(\frac{h}{l}+\sin\theta\right)\sin^2\theta}; \quad E_2^c = E\left(\frac{t}{l}\right)^3 \frac{\left(\frac{h}{l}+\sin\theta\right)}{\cos^3\theta}$$

$$v_{12}^c = \frac{\cos^2\theta}{\left(\frac{h}{l}+\sin\theta\right)\sin\theta}; \quad v_{21} = \frac{v_{12}E_2}{E_1}, \quad G_{12}^c = E\left(\frac{t}{l}\right)^3 \frac{\left(\frac{h}{l}+\sin\theta\right)}{\left(\frac{h}{l}\right)^2\left(1+2\frac{h}{l}\right)\cos\theta}$$

$$G_{13}^c = G_l^t \frac{\cos\theta}{\frac{h}{l}+\sin\theta}; \quad G_{23}^c = G_l^t \frac{1+2\sin^2\theta}{2\cos\theta\left(\frac{h}{l}+\sin\theta\right)}; \quad \rho_c = \rho \frac{t/l(h/l+2)}{2\cos\theta(h/l+\sin\theta)} \quad (2)$$

where symbol "c" represents core material, E, G and ρ are Young's moduli, shear moduli and mass density of the origin material.

The effect of geometry of the double curves shallow shells with negative Poisson's ratio v_{12} at the limited of small deformation is presented in Table 1 for the combinations of θ and $\frac{h}{l}$. From Table 1, it can be seen that Poisson's ratio v_{12} increases when geometric parameters of $\frac{h}{l}$ increases and vice versa, similarly geometric parameters of θ increases, Poisson's ratio v_{12} decreases and vice versa.

3. Theoretical formulation

In the present study, the third order shear deformation theory (TSDT) is used to derive the governing equations and determine the blast load of the composite double curved shallow shell with negative Poisson's ratio in auxetic honeycombs.

The relationship of strain-displacement based on Reddy's third order shear deformation theory [31]

$$\begin{pmatrix} \varepsilon_x \\ \varepsilon_y \\ \gamma_{xy} \end{pmatrix} = \begin{pmatrix} \varepsilon_x^0 \\ \varepsilon_y^0 \\ \gamma_{xy}^0 \end{pmatrix} + z \begin{pmatrix} k_x^1 \\ k_y^1 \\ k_{xy}^1 \end{pmatrix} + z^3 \begin{pmatrix} k_x^3 \\ k_y^3 \\ k_{xy}^3 \end{pmatrix}, \quad \begin{pmatrix} \gamma_{xz} \\ \gamma_{yz} \end{pmatrix} = \begin{pmatrix} \gamma_{xz}^0 \\ \gamma_{yz}^0 \end{pmatrix} + z^2 \begin{pmatrix} k_{xz}^2 \\ k_{yz}^2 \end{pmatrix}, \quad (3)$$

Table 1
Poisson's ratio v_{12} in auxetic honeycombs of the double curves shallow shells at the limited value of small deformation.

	$\frac{h}{l}=1$	$\frac{h}{l}=1.5$	$\frac{h}{l}=2$	$\frac{h}{l}=2.5$	$\frac{h}{l}=3$
$\theta=-35$	−2.7434	−1.2628	−0.8201	−0.6073	−0.4821
$\theta=-45$	−2.4142	−0.8918	−0.5469	−0.3944	−0.3084
$\theta=-50$	−2.3054	−0.7349	−0.4371	−0.3111	−0.2414
$\theta=-60$	−2.1547	−0.4553	−0.3401	−0.1767	−0.1353
$\theta=-75$	−2.0353	−0.1299	−0.0671	−0.0452	−0.0341

in which

$$\begin{pmatrix} k_x^1 \\ k_y^1 \\ k_{xy}^1 \end{pmatrix} = \begin{pmatrix} \frac{\partial\phi_x}{\partial x} \\ \frac{\partial\phi_y}{\partial y} \\ \frac{\partial\phi_x}{\partial y}+\frac{\partial\phi_y}{\partial x} \end{pmatrix}, \quad \begin{pmatrix} k_x^3 \\ k_y^3 \\ k_{xy}^3 \end{pmatrix} = -c_1 \begin{pmatrix} \frac{\partial\phi_x}{\partial x}+\frac{\partial^2 w}{\partial x^2} \\ \frac{\partial\phi_y}{\partial y}+\frac{\partial^2 w}{\partial y^2} \\ \frac{\partial\phi_x}{\partial y}+\frac{\partial\phi_y}{\partial x}+2\frac{\partial^2 w}{\partial x\partial y} \end{pmatrix}, \begin{pmatrix} \varepsilon_x^0 \\ \varepsilon_y^0 \\ \gamma_{xy}^0 \end{pmatrix}$$

$$= \begin{pmatrix} \frac{\partial u}{\partial x}-\frac{w}{R_x}+\frac{1}{2}\left(\frac{\partial w}{\partial x}\right)^2 \\ \frac{\partial v}{\partial y}-\frac{w}{R_y}+\frac{1}{2}\left(\frac{\partial w}{\partial y}\right)^2 \\ \frac{\partial u}{\partial y}+\frac{\partial v}{\partial x}+\frac{\partial w}{\partial x}\frac{\partial w}{\partial y} \end{pmatrix}, \begin{pmatrix} \gamma_{xz}^0 \\ \gamma_{yz}^0 \end{pmatrix} = \begin{pmatrix} \phi_x+\frac{\partial w}{\partial x} \\ \phi_y+\frac{\partial w}{\partial y} \end{pmatrix}, \begin{pmatrix} k_{xz}^2 \\ k_{yz}^2 \end{pmatrix} = -3c_1 \begin{pmatrix} \phi_x+\frac{\partial w}{\partial x} \\ \phi_y+\frac{\partial w}{\partial y} \end{pmatrix},$$

$$(4)$$

here $\varepsilon_x, \varepsilon_y$ are normal strain, $c_1 = \frac{4}{3h^2}$, u, v are displacement components along the x, y directions, ϕ_x, ϕ_y are the slope rotations in the (x,z) and (x,y) planes, γ_{xy} is the in-plane shear strain and γ_{xz}, γ_{yz} are the transverse shear deformations, k_x, k_y, k_{xy} are curvatures of the double curves shell.

Hooke's law for the double curves shallow shells with negative Poisson's ratio in auxetic honeycombs is defined as follows.

$$\begin{Bmatrix} \sigma_x^T \\ \sigma_y^T \\ \sigma_{xy}^T \end{Bmatrix} = \begin{bmatrix} Q_{11}^T & Q_{12}^T & 0 \\ Q_{12}^T & Q_{22}^T & 0 \\ 0 & 0 & Q_{66}^T \end{bmatrix} \begin{Bmatrix} \varepsilon_x \\ \varepsilon_y \\ \gamma_{xy} \end{Bmatrix}, \quad \begin{Bmatrix} \sigma_{yz}^T \\ \sigma_{xz}^T \end{Bmatrix} = \begin{bmatrix} Q_{44}^T & 0 \\ 0 & Q_{55}^T \end{bmatrix} \begin{Bmatrix} \gamma_{yz} \\ \gamma_{xz} \end{Bmatrix}$$

$$\begin{Bmatrix} \sigma_x^C \\ \sigma_y^C \\ \sigma_{xy}^C \end{Bmatrix} = \begin{bmatrix} Q_{11}^C & Q_{12}^C & 0 \\ Q_{12}^C & Q_{22}^C & 0 \\ 0 & 0 & Q_{66}^C \end{bmatrix} \begin{Bmatrix} \varepsilon_x \\ \varepsilon_y \\ \gamma_{xy} \end{Bmatrix}, \quad \begin{Bmatrix} \sigma_{yz}^C \\ \sigma_{xz}^C \end{Bmatrix} = \begin{bmatrix} Q_{44}^C & 0 \\ 0 & Q_{55}^C \end{bmatrix} \begin{Bmatrix} \gamma_{yz} \\ \gamma_{xz} \end{Bmatrix}$$

$$\begin{Bmatrix} \sigma_x^B \\ \sigma_y^B \\ \sigma_{xy}^B \end{Bmatrix} = \begin{bmatrix} Q_{11}^T & Q_{12}^T & 0 \\ Q_{12}^T & Q_{22}^T & 0 \\ 0 & 0 & Q_{66}^T \end{bmatrix} \begin{Bmatrix} \varepsilon_x \\ \varepsilon_y \\ \gamma_{xy} \end{Bmatrix}, \quad \begin{Bmatrix} \sigma_{yz}^B \\ \sigma_{xz}^B \end{Bmatrix} = \begin{bmatrix} Q_{44}^T & 0 \\ 0 & Q_{55}^T \end{bmatrix} \begin{Bmatrix} \gamma_{yz} \\ \gamma_{xz} \end{Bmatrix}$$

$$(5)$$

where above index T, C, B stand for Top outer skin, Core material, Bottom outer skin respectively.

$$Q_{11}^C = \frac{E_1^C}{1-v_{12}^C v_{21}^C}, \quad Q_{12}^C = \frac{v_{12}^C E_2^C}{1-v_{12}^C v_{21}^C}, \quad Q_{22}^C = \frac{E_2^C}{1-v_{12}^C v_{21}^C}, \quad Q_{66}^C = G_{12}^C, \quad Q_{44}^C$$

$$= G_{23}^C, \quad Q_{55}^C = G_{13}^C$$

$$Q_{11}^T = Q_{22}^T = \frac{E}{1-v^2}, \quad Q_{12}^T = \frac{vE}{1-v^2}, \quad Q_{66}^T = Q_{44}^T = Q_{55}^T = \frac{E}{2(1+v)} \quad (6)$$

The forces and moments of the double curves shallow shells can be expressed in terms of stress components across the double curves shallow shells thickness as

$$(N_i, M_i, P_i) = \int_{-\frac{h_2}{2}-h_3}^{-\frac{h_2}{2}} \sigma_i^B(1,z,z^3)dz + \int_{-\frac{h_2}{2}}^{\frac{h_2}{2}} \sigma_i^C(1,z,z^3)dz$$

$$\quad + \int_{\frac{h_2}{2}}^{\frac{h_2}{2}+h_1} \sigma_i^T(1,z,z^3)dz, i = x,y,xy$$

$$(Q_i, K_i) = \int_{-\frac{h_2}{2}-h_3}^{-\frac{h_2}{2}} \sigma_{iz}^B(1,z^2)dz + \int_{-\frac{h_2}{2}}^{\frac{h_2}{2}} \sigma_{iz}^C(1,z^2)dz + \int_{\frac{h_2}{2}}^{\frac{h_2}{2}+h_1} \sigma_{iz}^T(1,z^2)dz, i$$

$$= x,y$$

$$(7)$$

Substitution of Eqs. (3) into Eqs. (5) then take the result into Eqs. (7) gives the constitutive relations as

$$N_x = A_{11}\varepsilon_x^0 + A_{12}\varepsilon_y^0 + A_{13}k_x^1 + A_{14}k_y^1 + A_{15}k_x^3 + A_{16}k_y^3$$

$$N_y = A_{21}\varepsilon_x^0 + A_{22}\varepsilon_y^0 + A_{23}k_x^1 + A_{24}k_y^1 + A_{25}k_x^3 + A_{26}k_y^3$$

$$N_{xy} = A_{33}\gamma_{xy}^0 + A_{36}k_{xy}^1 + A_{39}k_{xy}^3$$

$$M_x = B_{11}\varepsilon_x^0 + B_{12}\varepsilon_y^0 + B_{13}k_x^1 + B_{14}k_y^1 + B_{15}k_x^3 + B_{16}k_y^3$$

$$M_y = B_{21}\varepsilon_x^0 + B_{22}\varepsilon_y^0 + B_{23}k_x^1 + B_{24}k_y^1 + B_{25}k_x^3 + B_{26}k_y^3$$

$$M_{xy} = B_{33}\gamma_{xy}^0 + B_{36}k_{xy}^1 + B_{39}k_{xy}^3$$

$$P_x = C_{11}\varepsilon_x^0 + C_{12}\varepsilon_y^0 + C_{13}k_x^1 + C_{14}k_y^1 + C_{15}k_x^3 + C_{16}k_y^3$$

$$P_y = C_{21}\varepsilon_x^0 + C_{22}\varepsilon_y^0 + C_{23}k_x^1 + C_{24}k_y^1 + C_{25}k_x^3 + C_{26}k_y^3$$

$$P_{xy} = C_{33}\gamma_{xy}^0 + C_{36}k_{xy}^1 + C_{39}k_{xy}^3$$

$$Q_x = D_{11}\gamma_{xz}^0 + D_{12}k_{xz}^2;$$

$$Q_y = D_{21}\gamma_{yz}^0 + D_{22}k_{yz}^2;$$

$$K_x = E_{11}\gamma_{xz}^0 + E_{12}k_{xz}^2;$$

$$K_y = E_{21}\gamma_{yz}^0 + E_{22}k_{yz}^2 \tag{8}$$

where $A_{ij}, B_{ij}, C_{ij}, D_{ij}, E_{ij}$ with $i = 1,2$ and $j = 1,2,3,4,5,6$ can be taken from Appendix A

Based on the TSDT, the nonlinear motion equations of the double curves shallow shells are defined by [31]

$$N_{x,x} + N_{xy,y} = \overline{I_1}\frac{\partial^2 u}{\partial t^2} + \overline{I_2}\frac{\partial^2 \phi_x}{\partial t^2} - \overline{I_3}\frac{\partial^3 w}{\partial t^2 \partial x} \tag{9a}$$

$$N_{xy,x} + N_{y,y} = \overline{I_1^*}\frac{\partial^2 v}{\partial t^2} + \overline{I_2^*}\frac{\partial^2 \phi_y}{\partial t^2} - \overline{I_3^*}\frac{\partial^3 w}{\partial t^2 \partial y} \tag{9b}$$

$$Q_{x,x} + Q_{y,y} - 3c_1(K_{x,x} + K_{y,y}) + c_1(P_{x,xx} + 2P_{xy,xy} + P_{y,yy}) + \frac{N_x}{R_x} + \frac{N_y}{R_y} + q + N_x w_{xx}$$
$$+ 2N_{xy}w_{xy} + N_y w_{yy} - k_1 w + k_2 \nabla^2 w = I_1\frac{\partial^2 w}{\partial t^2} + 2\varepsilon I_1\frac{\partial w}{\partial t} + \overline{I_3}\frac{\partial^3 u}{\partial t^2 \partial x} + \overline{I_5}\frac{\partial^3 \phi_x}{\partial t^2 \partial x}$$
$$+ \overline{I_3^*}\frac{\partial^3 v}{\partial t^2 \partial y} + \overline{I_5^*}\frac{\partial^3 \phi_y}{\partial t^2 \partial y} - c_1^2 I_7\left(\frac{\partial^4 w}{\partial t^2 \partial x^2} + \frac{\partial^4 w}{\partial t^2 \partial y^2}\right) \tag{9c}$$

$$M_{x,x} + M_{xy,y} - Q_x + 3c_1 K_x - c_1(P_{x,x} + P_{xy,y}) = \overline{I_2}\frac{\partial^2 u}{\partial t^2} + \overline{I_4}\frac{\partial^2 \phi_x}{\partial t^2} - \overline{I_5}\frac{\partial^3 w}{\partial t^2 \partial x} \tag{9d}$$

$$M_{xy,x} + M_{y,y} - Q_y + 3c_1 K_y - c_1(P_{xy,x} + P_{y,y}) = \overline{I_2^*}\frac{\partial^2 v}{\partial t^2} + \overline{I_4^*}\frac{\partial^2 \phi_y}{\partial t^2} - \overline{I_5^*}\frac{\partial^3 w}{\partial t^2 \partial y} \tag{9e}$$

where

$$\overline{I_1} = I_1 + \frac{2I_2}{R_x}, \quad \overline{I_1^*} = I_1 + \frac{2I_2}{R_y}, \quad \overline{I_2} = I_2 + \frac{I_3}{R_x} - c_1 I_4 - \frac{c_1 I_5}{R_x}, \quad \overline{I_2^*}$$

$$= I_2 + \frac{I_3}{R_y} - c_1 I_4 - \frac{c_1 I_5}{R_y}, \quad \overline{I_3} = c_1 I_4 + \frac{c_1 I_5}{R_x}$$

$$\overline{I_3^*} = c_1 I_4 + \frac{c_1 I_5}{R_y}, \quad \overline{I_4} = \overline{I_4^*} = I_3 - 2c_1 I_5 + c_1^2 I_7, \quad \overline{I_5} = \overline{I_5^*} = c_1 I_5 - c_1^2 I_7$$

$$(I_1, I_2, I_3, I_4, I_5, I_7) = \int_{-\frac{h_2}{2}-h_3}^{\frac{h_2}{2}}\rho^B z^i dz + \int_{\frac{h_2}{2}}^{\frac{h_2}{2}}\rho^C z^i dz + \int_{\frac{h_2}{2}}^{\frac{h_2}{2}+h_1}\rho^T z^i dz, \quad (i = 0,1,2,3,4,6)$$

The Airy stress function $f(x,y,t)$ is chosen as.

$$N_x = \frac{\partial^2 f}{\partial y^2}, N_y = \frac{\partial^2 f}{\partial x^2}, N_{xy} = -\frac{\partial^2 f}{\partial x \partial y}. \tag{10}$$

Combine (9a), (9b) and the stress function (10) we got

$$\frac{\partial^2 u}{\partial t^2} = -\frac{\overline{I_2}}{\overline{I_1}}\frac{\partial^2 \phi_x}{\partial t^2} + \frac{\overline{I_3}}{\overline{I_1}}\frac{\partial^3 w}{\partial t^2 \partial x} \tag{11a}$$

$$\frac{\partial^2 v}{\partial t^2} = -\frac{\overline{I_2^*}}{\overline{I_1^*}}\frac{\partial^2 \phi_y}{\partial t^2} + \frac{\overline{I_3^*}}{\overline{I_1^*}}\frac{\partial^3 w}{\partial t^2 \partial y} \tag{11b}$$

From the equation (8), we can rewrite $\varepsilon_x^0, \varepsilon_y^0, \gamma_{xy}^0$ as

$$\varepsilon_x^0 = A_{11}^* k_x^1 + A_{12}^* k_y^1 + A_{13}^* k_x^3 + A_{14}^* k_y^3 + A_{15}^* N_x + A_{16}^* N_y$$

$$\varepsilon_y^0 = A_{21}^* k_x^1 + A_{22}^* k_y^1 + A_{23}^* k_x^3 + A_{24}^* k_y^3 + A_{25}^* N_y + A_{26}^* N_x$$

$$\gamma_{xy}^0 = A_{33}^* N_{xy} + A_{36}^* k_{xy}^1 + A_{39}^* k_{xy}^3 \tag{12}$$

in which the coefficient $A_{ij}^*(i = 1,2; j = 1,2,3,4,5,6)$ are in Appendix B

Setting the Airy stress function (10) and the express (4) into the equation (12), we can rewrite the Eqs. (12) as follows.

$$\varepsilon_x^0 = A_{11}^* \phi_{x,x} + A_{12}^* \phi_{y,y} - c_1 A_{13}^*(\phi_{x,x} + w_{xx}) - c_1 A_{14}^*(\phi_{y,y} + w_{yy}) + A_{15}^* f_{yy}$$
$$+ A_{16}^* f_{xx}$$

$$\varepsilon_y^0 = A_{21}^* \phi_{x,x} + A_{22}^* \phi_{y,y} - c_1 A_{23}^*(\phi_{x,x} + w_{xx}) - c_1 A_{24}^*(\phi_{y,y} + w_{yy}) + A_{25}^* f_{xx}$$
$$+ A_{26}^* f_{yy}$$

$$\gamma_{xy}^0 = -A_{33}^* f_{xy} + A_{36}^*(\phi_{x,y} + \phi_{y,x}) - c_1 A_{39}^*(\phi_{x,y} + \phi_{y,x} + 2w_{xy}) \tag{13}$$

The geometrical compatibility equation for an imperfect double curves shell can be derived as [22–25]. Here, the imperfection function $w^*(x,y)$ represents initial small deviation of the shell surface from perfectly configuration.

$$\varepsilon_{x,yy}^0 + \varepsilon_{y,xx}^0 - \gamma_{xy,xy}^0 = w_{xy}^2 - w_{xx}w_{yy} + 2w_{xy}w_{xy}^* - w_{xx}w_{yy}^* - w_{yy}w_{xx}^* - \frac{w_{yy}}{R_x}$$
$$- \frac{w_{xx}}{R_y} \tag{14}$$

Substituting the expresses (13) into the equation (14), we receive

$$\overline{A_{21}^*}\frac{\partial^3 \phi_x}{\partial x^3} + \overline{A_{22}^*}\frac{\partial^3 \phi_y}{\partial y^3} + \overline{A_{23}^*}\frac{\partial^3 \phi_y}{\partial x^2 \partial y} + \overline{A_{24}^*}\frac{\partial^3 \phi_x}{\partial x \partial y^2} + \overline{A_{25}^*}\frac{\partial^4 w}{\partial x^4} + \overline{A_{26}^*}\frac{\partial^4 w}{\partial x^2 \partial y^2}$$
$$+ \overline{A_{27}^*}\frac{\partial^4 w}{\partial y^4} + A_{15}^* f_{yyyy} + \overline{A_{28}^*}f_{xxyy} + A_{25}^* f_{xxxx} = w_{xy}^2 - w_{xx}w_{yy}$$
$$+ 2w_{xy}w_{xy}^* - w_{xx}w_{yy}^* - w_{yy}w_{xx}^* - \frac{w_{yy}}{R_x} - \frac{w_{xx}}{R_y} \tag{15}$$

where

$$\overline{A_{21}^*} = (A_{21}^* - c_1 A_{23}^*); \quad \overline{A_{22}^*} = (A_{12}^* - c_1 A_{14}^*); \quad \overline{A_{23}^*} = (A_{22}^* - A_{36}^* - c_1 A_{24}^* + c_1 A_{39}^*);$$

$$\overline{A_{24}^*} = (A_{11}^* - A_{36}^* - c_1 A_{13}^* + c_1 A_{39}^*); \quad \overline{A_{25}^*} = (-c_1 A_{23}^*); \quad \overline{A_{26}^*}$$
$$= (-c_1 A_{13}^* - c_1 A_{24}^* + 2c_1 A_{39}^*);$$

$$\overline{A_{27}^*} = (-c_1 A_{14}^*); \overline{A_{28}^*} = (A_{16}^* + A_{26}^* + A_{33}^*);$$

Taking Eqs. (10) and (11) into account expressions (9c,d,e), yields a system of equations

$$Q_{x,x} + Q_{y,y} - 3c_1(K_{x,x} + K_{y,y}) + c_1(P_{x,xx} + 2P_{xy,xy} + P_{y,yy}) + \frac{f_{yy}}{R_x} + \frac{f_{xx}}{R_y} + q + f_{yy}w_{xx}$$
$$- 2f_{xy}w_{xy} + f_{xx}w_{yy} - k_1 w + k_2 \nabla^2 w = I_1\frac{\partial^2 w}{\partial t^2} + 2\varepsilon I_1\frac{\partial w}{\partial t} + \overline{\overline{I_5}}\frac{\partial^3 \phi_x}{\partial t^2 \partial x} + \overline{\overline{I_5^*}}\frac{\partial^3 \phi_y}{\partial t^2 \partial y}$$
$$+ \overline{\overline{I_7}}\frac{\partial^4 w}{\partial t^2 \partial x^2} + \overline{\overline{I_7^*}}\frac{\partial^4 w}{\partial t^2 \partial y^2} \tag{16a}$$

$$M_{x,x} + M_{xy,y} - Q_x + 3c_1 K_x - c_1(P_{x,x} + P_{xy,y}) = \overline{\overline{I_3}}\frac{\partial^2 \phi_x}{\partial t^2} - \overline{\overline{I_5}}\frac{\partial^3 w}{\partial t^2 \partial x} \tag{16b}$$

$$M_{xy,x} + M_{y,y} - Q_y + 3c_1 K_y - c_1(P_{xy,x} + P_{y,y}) = \overline{\overline{I_3^*}}\frac{\partial^2 \phi_y}{\partial t^2} - \overline{\overline{I_5^*}}\frac{\partial^3 w}{\partial t^2 \partial y} \tag{16c}$$

where

$$\overline{\overline{I_5}} = \overline{I_5} - \frac{\overline{I_3}\overline{I_2}}{\overline{I_1}}, \quad \overline{\overline{I_7}} = \frac{(\overline{I_3})^2}{\overline{I_1}} - c_1^2 I_7, \quad \overline{\overline{I_5^*}} = \overline{I_5^*} - \frac{\overline{I_3^*}\overline{I_2^*}}{\overline{I_1^*}}, \quad \overline{\overline{I_7^*}} = \frac{(\overline{I_3^*})^2}{\overline{I_1^*}} - c_1^2 I_7, \quad \overline{\overline{I_3}}$$
$$= \overline{I_4} - \frac{(\overline{I_2})^2}{\overline{I_1}}, \quad \overline{\overline{I_3^*}} = \overline{I_4^*} - \frac{(\overline{I_2^*})^2}{\overline{I_1^*}}$$

By substituting Eq. (4) into Eq. (8) and then into Eqs. (16), the system of motion Eqs. (16) are rewritten as follows

$H_{11}(\phi_x) + H_{12}(\phi_y) + H_{13}(w) + H_{14}(f) + H_{15}(w,f) + H_{13}^*(w^*) + H_{15}^*(w^*,f)$

$\quad + q = I_1\dfrac{\partial^2 w}{\partial t^2} + 2\varepsilon I_1\dfrac{\partial w}{\partial t} + \overline{\overline{I_5}}\dfrac{\partial^3\phi_x}{\partial t^2\partial x} + \overline{\overline{I_5}}\dfrac{\partial^3\phi_y}{\partial t^2\partial y} + \overline{\overline{I_7}}\dfrac{\partial^4 w}{\partial t^2\partial x^2} + \overline{\overline{I_7}}\dfrac{\partial^4 w}{\partial t^2\partial y^2}$

$H_{21}(\phi_x) + H_{22}(\phi_y) + H_{23}(w) + H_{24}(f) + H_{23}^*(w^*) = \overline{I_3}\dfrac{\partial^2\phi_x}{\partial t^2} - \overline{I_5}\dfrac{\partial^3 w}{\partial t^2\partial x}$

$H_{31}(\phi_x) + H_{32}(\phi_y) + H_{33}(w) + H_{34}(f) + H_{33}^*(w^*) = \overline{I_3^*}\dfrac{\partial^2\phi_y}{\partial t^2} - \overline{I_5^*}\dfrac{\partial^3 w}{\partial t^2\partial y}$

$$(17)$$

where

$H_{11}(\phi_x) = U_{11}\phi_{x,x} + U_{13}\phi_{x,xxx} + U_{14}\phi_{x,xyy}; \quad H_{12}(\phi_y) = U_{12}\phi_{y,y} + U_{15}\phi_{y,xxy}$
$\quad + U_{16}\phi_{y,yyy}$

$H_{13}(w) = U_{11}w_{,xx} + U_{12}w_{,yy} + U_{17}w_{,xxxx} + U_{18}w_{,xxyy} + U_{19}w_{,yyyy} - k_1 w$
$\quad + k_2\nabla^2 w$

$H_{14}(f) = U_{110}f_{,xxxx} + U_{111}f_{,xxyy} + U_{112}f_{,yyyy} + \dfrac{f_{,yy}}{R_x} + \dfrac{f_{,xx}}{R_y};; \quad H_{15}(w,f)$
$\quad = f_{,yy}w_{,xx} - 2f_{,xy}w_{,xy} + f_{,xx}w_{,yy}$

$H_{21}(\phi_x) = U_{21}\phi_x + U_{22}\phi_{x,xx} + U_{23}\phi_{x,yy}; \quad H_{22}(\phi_y) = U_{24}\phi_{y,xy};$

$H_{23}(w) = U_{21}w_{,x} + U_{25}w_{,xxx} + U_{26}w_{,xyy}; \quad H_{24}(f) = U_{27}f_{,xyy} + U_{28}f_{,xxx};$

$H_{31}(\phi_x) = U_{31}\phi_{x,xy}; \quad H_{32}(\phi_y) = U_{32}\phi_y + U_{33}\phi_{y,xx} + U_{34}\phi_{y,yy};$

$H_{33}(w) = U_{32}w_{,y} + U_{35}w_{,xxy} + U_{36}w_{,yyy}; \quad H_{34}(f) = U_{37}f_{,yyy} + U_{38}f_{,xxy};$

$H_{13}^*(w^*) = U_{11}w_{,xx}^* + U_{12}w_{,yy}^* + U_{17}w_{,xxxx}^* + U_{18}w_{,xxyy}^* + U_{19}w_{,yyyy}^*$

$H_{15}^*(w^*,f) = f_{,yy}w_{,xx}^* - 2f_{,xy}w_{,xy}^* + f_{,xx}w_{,yy}^*, H_{23}^*(w^*) = U_{21}w_{,x}^* + U_{25}w_{,xxx}^*$
$\quad + U_{26}w_{,xyy}^*$

$H_{33}^*(w^*) = U_{32}w_{,y}^* + U_{35}w_{,xxy}^* + U_{36}w_{,yyy}^*$

here, the coefficient U_{ijk} is in Appendix C

Equations (17) and Eq. (15) are nonlinear equations in terms of variables w, ϕ_x, ϕ_y and f. They are used to investigate the nonlinear vibration and dynamic stability of the double curved shallow shell with negative Poisson's ratio in auxetic honeycombs core layer using the TSDT.

4. Nonlinear dynamic analysis

The edges of the shell are freely movable (FM), subjected to the blast load q and the compression load P_x and P_y (Pascal) at edges $x = 0, a$ and $y = 0, b$, respectively [22–25]

$w = M_x = N_{xy} = 0, N_x = N_{x0}$ at $x = 0, a$
$w = M_y = N_{xy} = 0, N_y = N_{y0}$ at $y = 0, b$

$$(18)$$

The following approximate solution is seen to satisfy the differential equations and the boundary conditions

$w(x,y,t) = W(t)\sin\alpha x\sin\beta y$
$\phi_x(x,y,t) = \Phi_x(t)\cos\alpha x\sin\beta y$
$\phi_y(x,y,t) = \Phi_y(t)\sin\alpha x\cos\beta y$

$$(19)$$

where $\alpha = m\pi/a, \beta = n\pi/b; m, n$ are odd natural numbers representing the number of half waves in the x and y directions, respectively; and $W(t), \Phi_x, \Phi_y$ are the time dependent amplitudes.

The initial imperfection of the shell is supposed to have the form like the shell deflection, i.e.

$w^*(x,y) = W_0\sin\alpha x\sin\beta y$

$$(20)$$

The approximate solution of the Eqs. (15) and (17) is assumed as

$f(x,y,t) = Y_1(t)\cos 2\alpha x + Y_2(t)\cos 2\beta y + Y_3(t)\sin\alpha x\sin\beta y + \dfrac{1}{2}N_{x0}y^2$
$\quad + \dfrac{1}{2}N_{y0}x^2$

$$(21)$$

the coefficients Y_1, Y_2, Y_3 are given by substitute the approximate solutions. (19) and (20) into the expression (15) lead to

$Y_1(t) = H_1 W(W + 2W_0) \quad Y_2(t) = H_2 W(W + 2W_0) \quad Y_3(t)$
$\quad = H_3\Phi_x(t) + H_4\Phi_y(t) + H_5 W$

$$(22)$$

where

$H_0 = (A_{25}^*\alpha^4 + \overline{A_{28}^*}\alpha^2\beta^2 + A_{15}^*\beta^4); \quad H_1 = \dfrac{\alpha^2\beta^2}{2A_{25}^*(2\alpha)^4}; H_2 = \dfrac{\alpha^2\beta^2}{2A_{15}^*(2\beta)^4};$

$H_3 = -(\overline{A_{21}^*}\alpha^3 + \overline{A_{24}^*}\alpha\beta^2)/H_0; \quad H_4 = -(\overline{A_{22}^*}\beta^3 + \overline{A_{23}^*}\alpha^2\beta)/H_0;$

$H_5 = -\left(\overline{A_{25}^*}\alpha^4 + \overline{A_{26}^*}\alpha^2\beta^2 + \overline{A_{27}^*}\beta^4 - \dfrac{\beta^2}{R_x} - \dfrac{\alpha^2}{R_y}\right)/H_0$

Replacing Eqs. (19), (20) and (21) into the equations of motion (17) and then applying Galerkin method, we obtain

$J_{11}\Phi_x + J_{12}\Phi_y + J_{13}W + J_{14}\Phi_x(W + W_0) + J_{15}\Phi_y(W + W_0) + J_{16}(W + W_0)$
$\quad + J_{17}W(W + W_0) + J_{18}W(W + 2W_0) + J_{19}W(W + W_0)(W + 2W_0)$
$\quad + \dfrac{16}{\pi^2}\left(\dfrac{N_{x0}}{R_x} + \dfrac{N_{y0}}{R_y}\right) + \dfrac{16}{\pi^2}q(t) = I_1\dfrac{\partial^2 W}{\partial t^2} + 2\varepsilon I_1\dfrac{\partial W}{\partial t} - \alpha\overline{\overline{I_5}}\dfrac{\partial^2\Phi_x}{\partial t^2} - \beta\overline{\overline{I_5}}\dfrac{\partial^2\Phi_y}{\partial t^2}$

$J_{21}\Phi_x + J_{22}\Phi_y + J_{23}W + J_{24}(W + W_0) + J_{25}W(W + 2W_0)$
$\quad = \overline{I_3}\dfrac{\partial^2\Phi_x}{\partial t^2} - \alpha\overline{I_5}\dfrac{\partial^2 W}{\partial t^2}$

$J_{31}\Phi_x + J_{32}\Phi_y + J_{33}W + J_{34}(W + W_0) + J_{35}W(W + 2W_0)$
$\quad = \overline{I_3^*}\dfrac{\partial^2\Phi_y}{\partial t^2} - \beta\overline{I_5^*}\dfrac{\partial^2 W}{\partial t^2}$

$$(23)$$

in which, the factors $J_{ij}(i = 1,2,3; j = \overline{1,9})$ are shown in Appendix D

In which, the compression load follows as [22–25]

$N_{x0} = -P_x h; \quad N_{y0} = -P_y h$

$$(24)$$

The blast load $q(t)$ is a short–term load and is generated by an explosion or by a shock-wave disturbance produced by an aircraft flying at supersonic speed, or by a supersonic projectile, rocket or missile operating in its vicinity. It can be written as [16]

$q(t) = 1.8Ps_{max}\left(1 - \dfrac{t}{T_s}\right)exp\left(\dfrac{-bt}{T_s}\right)$

$$(25)$$

where the "1.8" factor accounts for the effects of a hemispherical blast, Ps_{max} is the maximum (or peak) static over-pressure, b is the parameter controlling the rate of wave amplitude decay and T_s is the parameter characterizing the duration of the blast pulse.

In the case without the blast load $q(t)$, the natural frequencies of the perfect shell are the smallest values of the axial, circumferential and radial directions, which can be defined solving the following determinant.

$\begin{vmatrix} J_{13} + J_{16} + I_1\omega^2 & J_{11} - \alpha\overline{I_5}\omega^2 & J_{12} - \beta\overline{I_5^*}\omega^2 \\ J_{23} + J_{24} - \alpha\overline{I_5}\omega^2 & J_{21} + \overline{I_3}\omega^2 & J_{22} \\ J_{33} + J_{34} - \beta\overline{I_5^*}\omega^2 & J_{31} & J_{32} + \overline{I_3^*}\omega^2 \end{vmatrix} = 0$

$$(26)$$

The system equations above describing the nonlinear vibration for imperfect auxetic double curved shallow shells on the foundation elastic with the edges of the shell are freely movable (FM), subjected to the blast load q and the compression load P_x, P_y (Pascal) at edges $x = 0, a$ and $y = 0, b$, respectively. By using the fourth order Runge-Kutta's method or Newmark's numerical integration method, we can solve the integral equation (23) with the initial conditions are chosen as $W(0) = 0$ and $\dot{W}(0) = 0$.
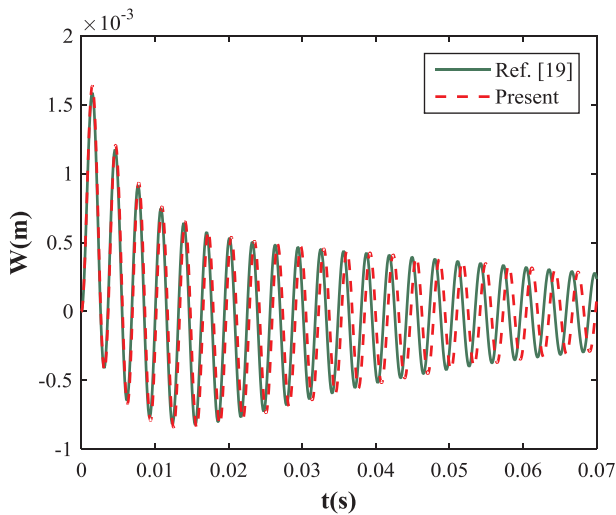
Fig. 4. The Comparison of nonlinear dynamic response of the FGM plate subjected to blast load with results of Ref [19].

5. Numerical results and discussion

5.1. Numerical verification

In order to verify the accuracy of the proposed formulas, Fig. 4 shows the comparison of the nonlinear dynamic response of plate (only made of ceramic) on the elastic foundations under blast load in this paper with the paper's result of Duc et al. [19]. In [19], Duc et al. studied of nonlinear dynamic response of FGM plate on the elastic foundation under blast load, when $N = 0$, FGM plate becomes purely made of ceramic. Fig. 5 compares nonlinear dynamic response of the double curves shallow shells with auxetic honeycombs subjected to blast load in present study (using TSDT) with the result of [15] (using FSDT).

The parameters in Fig. 4 are selected as follows

$$\frac{b}{a} = 1, \frac{b}{h} = 20, K_1 = 0.3 \text{ GPa/m}, K_2 = 0.02 \text{ GPa.m},$$

$$E = E_1^c = E_2^c = 384.43 \times 10^9 (0 \times T^{-1} + 1 - 3.07 \times 10^{-4}T$$
$$+ 2.160 \times 10^{-7}T^2 - 8.94 \times 10^{-11}T^3)\text{Pa}$$
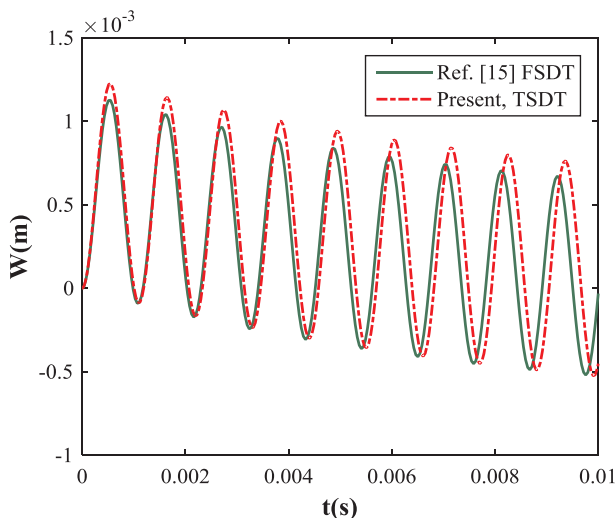
Fig. 5. The comparison of nonlinear dynamic response of the double curves shallow shells with auxetic honeycombs subjected to blast load in present study (using TSDT) with the result of [15] (using FSDT).

$$T = (300 + 350)K, \rho = \rho_c = 2370 \text{ kg/m}^3, G_{12}^c = G_{13}^c = G_{23}^c = G = \frac{E}{2(1 + \nu)}$$

To compare, the geometric parameters in the Fig. 5 is chosen follow the Ref. [15] as below

$$R_x = R_y = 6 \text{ m}; h_1 = h_3 = 0.00667 \text{ m}; h_2 = 0.02 \text{ m}; h = h_1 + h_2 + h_3; a/h$$
$$= 30; a = b; m = n = 1 t/l = 0.0138571; h/l = 2; \theta = -55^0; E$$
$$= 70 \text{ GPa}; G = 26 \text{ GPa}; \rho = 2702 \text{ kg/m}^3; \nu = 0.33$$

5.2. Nonlinear dynamic response

The effect of geometrical parameters of core material (cell angle and ratio $\frac{h}{l}$) on natural frequencies of sandwich plates with auxetic core is showed in Table 2. From Table 2, it can be seen that this effect does not follow any rule; which shows the complex behavior of sandwich plates with auxetic core when changing the geometrical parameters of the core material.

Fig. 6 illustrates the effect of damping on amplitude-time curves for nonlinear dynamic response of the double curved shallow shell with negative Poisson's ratio in core layer with three values of damping coefficient $\varepsilon = (0;5;10)$. From Fig. 6, we can see that when damping coefficient ε is increased, the curve becomes lower and vice versa.

Fig. 7 shows the effect of pre-loaded axial compression P_x on the nonlinear dynamic response ($\nu_{12} = -0.3401$). This figure also indicates that the nonlinear dynamic response amplitude of auxetic material of the double curved shallow shell with auxetic core increases when the value of the pre-loaded compressive force P_x increases.

Fig. 8 describes the nonlinear vibration of the nonlinear dynamic response of the double curved shallow shell with negative Poisson's ratio. Obviously, the amplitude of vibration will increase and lose the stability if the initial imperfection increases. We can see that the imperfect coefficient has a significant effect on the nonlinear dynamic response of the double curved shallow shell with negative Poisson's ratio.

Figs. 9 and 10 show the effects of the elastic foundations (linear Winkler foundation and Pasternak foundation) on the nonlinear dynamic response of the auxetic material of double curved shallow shell with negative Poisson's ratio under blast load ($\nu_{12} = -0.3401$). From the figures, it can be seen that the elastic foundations make the vibration amplitude of the auxetic material of the double curved shallow shell with negative Poisson's ratio reduce when increasing the coefficients of elastic foundations (k_1 and k_2). That shows the positive effect of elastic foundations. Furthermore, Winkler's elastic foundation (k_1) is weaker than Pasternak's foundation (k_2).

Fig. 11 shows the effect of parameter characterizing the duration of the blast pulse on nonlinear response of auxetic material of the double curved shallow shell with auxetic core with three values of $T_s = (0.005, 0.01, 0.02)$. From the figure, it can be seen that when the value of T_s is increased which makes the amplitude of nonlinear response increase and vice versa. At the same time, the time from $t = 0$ to amplitude of nonlinear response unchanged increases and vice versa.

Table 2
Effect of cell angle θ and ratio $\frac{h}{l}$ on natural frequencies $\omega(s^{-1})$ of the double curved shallow shells with negative Poisson's ratios in auxetic honeycombs.

	$\theta = -30°$	$\theta = -40°$	$\theta = -50°$	$\theta = -60°$	$\theta = -70°$
$h/l = 0.5$	1879.6	30402	21024	23706	18809
$h/l = 1$	10347	10869	10780	10916	3349.8
$h/l = 2$	11262	7675.6	3755.9	3273	4568.9
$h/l = 4$	3115.2	3400	4657.3	5087.5	5038.4
$h/l = 6$	3383.7	4616.8	5057.8	5139.2	4900.6
$h/l = 8$	4271.9	4892	5092.5	5039.6	4714.9
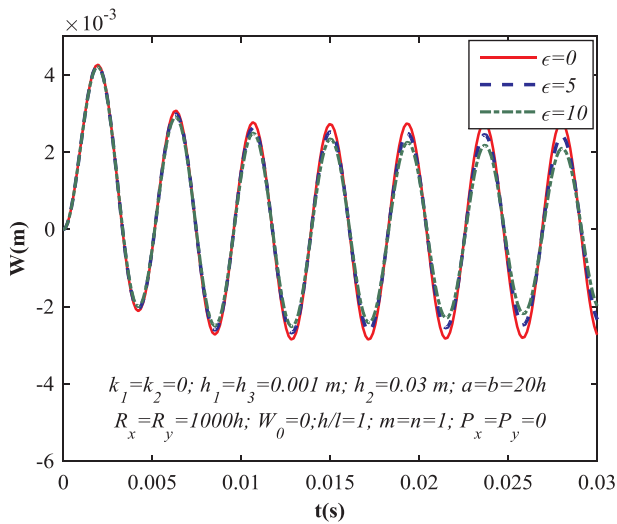
Fig. 6. Effects of ratio ε on the nonlinear dynamic response of the double curved shallow shell with negative Poisson's ratio under blast load.
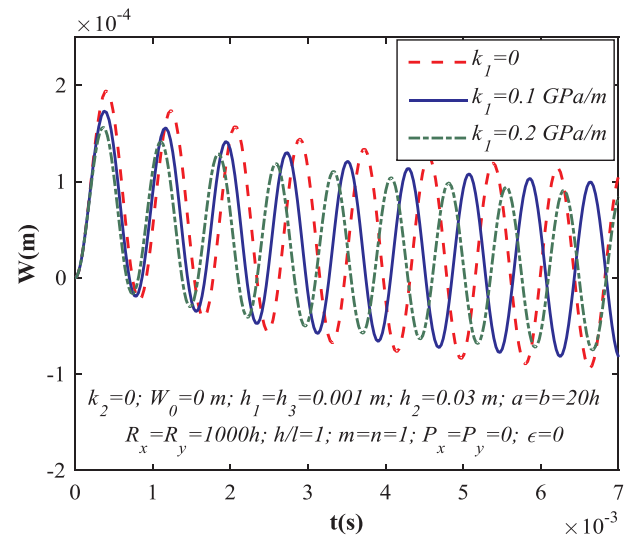
Fig. 9. Effects of coefficient k_1 on the nonlinear dynamic response of the double curved shallow shell with negative Poisson's ratio under blast load.
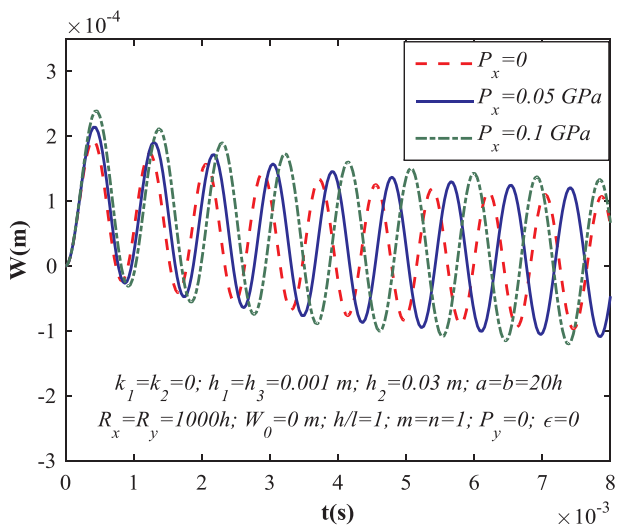
Fig. 7. Effects of coefficient P_x on the nonlinear dynamic response of the double curved shallow shell with negative Poisson's ratio under blast load.
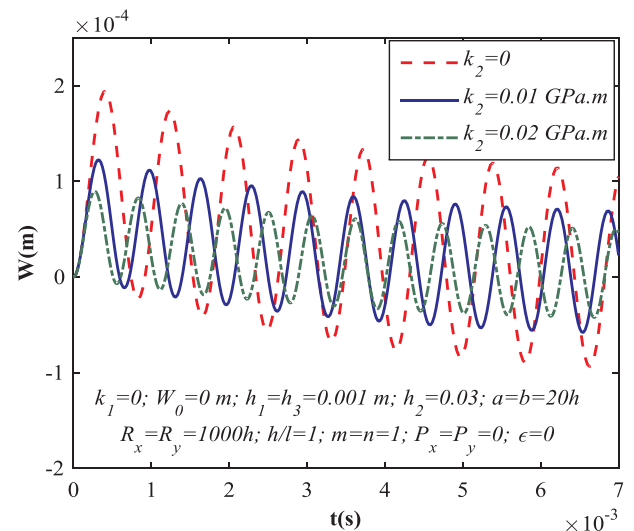
Fig. 10. Effects of coefficient k_2 on the nonlinear dynamic response of the double curved shallow shell with negative Poisson's ratio under blast load.

6. Conclusions

In the paper, the nonlinear dynamic response of the double curved shallow shells with negative Poisson's ratio under blast and mechanical loads and on elastic foundations is mainly studied. The analytical solution and the third order shear deformation theory are used to form the basic equations. By using the Galerkin method, the equation system of motion to determine dynamic response is found. The numerical results are investigated by the Runge–Kutta procedure.

Some special conclusions are obtained for the double curved shallow shells with negative Poisson's ratio to blast and mechanical loads:

- Build up the analytic method to analyze the nonlinear dynamical response of the double curved shallow shells with negative Poisson's ratio to blast and mechanical loads. From then, the authors find a new approach to research static and dynamic response for the double curved shallow shells with negative Poisson's ratio under blast and mechanical loads.

Fig. 8. Effects of coefficient $W_h = W_0/h$ on the nonlinear dynamic response of the double curved shallow shell with negative Poisson's ratio under blast load.
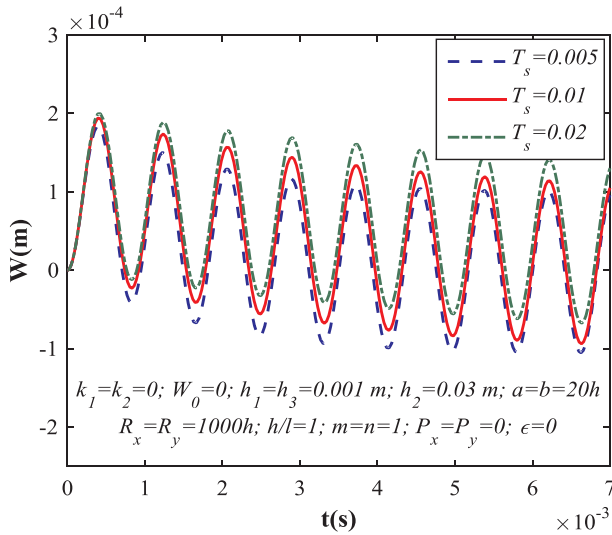
Fig. 11. Effect of parameter characterizing the duration of the blast pulse T_s on nonlinear response of the double curved shallow shell with negative Poisson's ratio.

geometrical properties, mechanical and elastic foundations on natural frequency and the nonlinear dynamic response of the double curved shallow shells with negative Poisson's ratio in auxetic honeycombs.

Conflict of interest statement

The authors declare no conflict of interest.

Funding

- The paper also analyses and discusses the effects of material and

Appendix A

$A_{11} = (h_3 Q_{11}^T + h_2 Q_{11}^C + h_1 Q_{11}^T); \quad A_{12} = (h_3 Q_{12}^T + h_2 Q_{12}^C + h_1 Q_{12}^T); \quad A_{13} = [h_1(h_1 + h_2) - h_3(h_2 + h_3)] Q_{11}^T;$

$A_{14} = [h_1(h_1 + h_2) - h_3(h_2 + h_3)] Q_{12}^T; \quad A_{15} = Q_{11}^T \left[\left(\frac{h_2}{2} + h_1 \right)^4 - \left(\frac{h_2}{2} + h_3 \right)^4 \right];$

$A_{16} = Q_{12}^T \left[\left(\frac{h_2}{2} + h_1 \right)^4 - \left(\frac{h_2}{2} + h_3 \right)^4 \right]; \quad A_{21} = (h_3 Q_{12}^T + h_2 Q_{12}^C + h_1 Q_{12}^T); \quad A_{22} = (h_3 Q_{22}^T + h_2 Q_{22}^C + h_1 Q_{22}^T);$

$A_{23} = [h_1(h_1 + h_2) - h_3(h_2 + h_3)] Q_{12}^T; \quad A_{24} = [h_1(h_1 + h_2) - h_3(h_2 + h_3)] Q_{22}^T;$

$A_{25} = Q_{12}^T \left[\left(\frac{h_2}{2} + h_1 \right)^4 - \left(\frac{h_2}{2} + h_3 \right)^4 \right]; \quad A_{26} = Q_{22}^T \left[\left(\frac{h_2}{2} + h_1 \right)^4 - \left(\frac{h_2}{2} + h_3 \right)^4 \right];$

$A_{33} = (Q_{66}^T h_3 + Q_{66}^C h_2 + Q_{66}^T h_1); \quad A_{36} = [h_1(h_1 + h_2) - h_3(h_2 + h_3)] Q_{66}^T;$

$A_{39} = Q_{66}^T \left[\left(\frac{h_2}{2} + h_1 \right)^4 - \left(\frac{h_2}{2} + h_3 \right)^4 \right];$

$B_{11} = [h_1(h_1 + h_2) - h_3(h_2 + h_3)] Q_{11}^T; \quad B_{12} = [h_1(h_1 + h_2) - h_3(h_2 + h_3)] Q_{12}^T;$

$B_{13} = \left[\frac{h_2^3}{4} Q_{11}^C + \left(\frac{h_2}{2} + h_3 \right)^3 Q_{11}^T - \frac{h_2^3}{4} Q_{11}^T + \left(\frac{h_2}{2} + h_1 \right)^3 Q_{11}^T \right];$

$B_{14} = \left[\frac{h_2^3}{4} Q_{12}^C + \left(\frac{h_2}{2} + h_3 \right)^3 Q_{12}^T - \frac{h_2^3}{4} Q_{12}^T + \left(\frac{h_2}{2} + h_1 \right)^3 Q_{12}^T \right];$

$B_{15} = \left[\frac{h_2^5}{16} Q_{11}^C + \left(\frac{h_2}{2} + h_3 \right)^5 Q_{11}^T - \frac{h_2^5}{16} Q_{11}^T + \left(\frac{h_2}{2} + h_1 \right)^5 Q_{11}^T \right];$

$B_{16} = \left[\frac{h_2^5}{16} Q_{12}^C + \left(\frac{h_2}{2} + h_3 \right)^5 Q_{12}^T - \frac{h_2^5}{16} Q_{12}^T + \left(\frac{h_2}{2} + h_1 \right)^5 Q_{12}^T \right]; \quad B_{21} = [h_1(h_1 + h_2) - h_3(h_2 + h_3)] Q_{12}^T;$

$B_{22} = [h_1(h_1 + h_2) - h_3(h_2 + h_3)] Q_{22}^T; \quad B_{23} = \left[\frac{h_2^3}{4} Q_{12}^C + \left(\frac{h_2}{2} + h_3 \right)^3 Q_{12}^T - \frac{h_2^3}{4} Q_{12}^T + \left(\frac{h_2}{2} + h_1 \right)^3 Q_{12}^T \right];$

$B_{24} = \left[\frac{h_2^3}{4} Q_{22}^C + \left(\frac{h_2}{2} + h_3 \right)^3 Q_{22}^T - \frac{h_2^3}{4} Q_{22}^T + \left(\frac{h_2}{2} + h_1 \right)^3 Q_{22}^T \right];$

$B_{25} = \left[\frac{h_2^5}{16} Q_{12}^C + \left(\frac{h_2}{2} + h_3 \right)^5 Q_{12}^T - \frac{h_2^5}{16} Q_{12}^T + \left(\frac{h_2}{2} + h_1 \right)^5 Q_{12}^T \right];$

$B_{26} = \left[\frac{h_2^5}{16} Q_{22}^C + \left(\frac{h_2}{2} + h_3 \right)^5 Q_{22}^T - \frac{h_2^5}{16} Q_{22}^T + \left(\frac{h_2}{2} + h_1 \right)^5 Q_{22}^T \right]; \quad B_{33} = [h_1(h_1 + h_2) - h_3(h_2 + h_3)] Q_{66}^T;$

$B_{36} = \left[\left(\frac{h_2}{2} + h_3 \right)^3 Q_{66}^T - \frac{h_2^3}{4} Q_{66}^T + \frac{h_2^3}{4} Q_{66}^C + \left(\frac{h_2}{2} + h_1 \right)^3 Q_{66}^T \right];$

$B_{39} = \left[\left(\frac{h_2}{2} + h_3 \right)^5 Q_{66}^T - \frac{h_2^5}{16} Q_{66}^T + \frac{h_2^5}{16} Q_{66}^C + \left(\frac{h_2}{2} + h_1 \right)^5 Q_{66}^T \right];$

$C_{11} = \left[\left(\frac{h_2}{2} + h_1 \right)^4 - \left(\frac{h_2}{2} + h_3 \right)^4 \right] Q_{11}^T; \quad C_{12} = \left[\left(\frac{h_2}{2} + h_1 \right)^4 - \left(\frac{h_2}{2} + h_3 \right)^4 \right] Q_{12}^T;$

$C_{13} = \left[\left(\frac{h_2}{2} + h_3 \right)^5 Q_{11}^T - \frac{h_2^5}{16} Q_{11}^T + \frac{h_2^5}{16} Q_{11}^C + \left(\frac{h_2}{2} + h_1 \right)^5 Q_{11}^T \right];$

$C_{14} = \left[\left(\frac{h_2}{2} + h_3 \right)^5 Q_{12}^T - \frac{h_2^5}{16} Q_{12}^T + \frac{h_2^5}{16} Q_{12}^C + \left(\frac{h_2}{2} + h_1 \right)^5 Q_{12}^T \right];$

$C_{15} = \left[\left(\frac{h_2}{2} + h_3 \right)^7 Q_{11}^T - \frac{h_2^7}{64} Q_{11}^T + \frac{h_2^7}{64} Q_{11}^C + \left(\frac{h_2}{2} + h_1 \right)^7 Q_{11}^T \right]; \quad C_{16} = \left[\left(\frac{h_2}{2} + h_3 \right)^7 Q_{12}^T - \frac{h_2^7}{64} Q_{12}^T + \frac{h_2^7}{64} Q_{12}^C + \left(\frac{h_2}{2} + h_1 \right)^7 Q_{12}^T \right]; \quad C_{21} = \left[\left(\frac{h_2}{2} + h_1 \right)^4 - \left(\frac{h_2}{2} + h_3 \right)^4 \right] Q_{12}^T;$

$C_{22} = \left[\left(\frac{h_2}{2} + h_1 \right)^4 - \left(\frac{h_2}{2} + h_3 \right)^4 \right] Q_{22}^T; \quad C_{23} = \left[\left(\frac{h_2}{2} + h_3 \right)^5 Q_{12}^T - \frac{h_2^5}{16} Q_{12}^T + \frac{h_2^5}{16} Q_{12}^C + \left(\frac{h_2}{2} + h_1 \right)^5 Q_{12}^T \right];$

$C_{24} = \left[\left(\frac{h_2}{2} + h_3 \right)^5 Q_{22}^T - \frac{h_2^5}{16} Q_{22}^T + \frac{h_2^5}{16} Q_{22}^C + \left(\frac{h_2}{2} + h_1 \right)^5 Q_{22}^T \right];$

$C_{25} = \left[\left(\frac{h_2}{2} + h_3 \right)^7 Q_{12}^T - \frac{h_2^7}{64} Q_{12}^T + \frac{h_2^7}{64} Q_{12}^C + \left(\frac{h_2}{2} + h_1 \right)^7 Q_{12}^T \right];$

$C_{26} = \left[\left(\frac{h_2}{2} + h_3 \right)^7 Q_{22}^T - \frac{h_2^7}{64} Q_{22}^T + \frac{h_2^7}{64} Q_{22}^C + \left(\frac{h_2}{2} + h_1 \right)^7 Q_{22}^T \right]; \quad C_{33} = \left[\left(\frac{h_2}{2} + h_1 \right)^4 - \left(\frac{h_2}{2} + h_3 \right)^4 \right] Q_{66}^T;$

$C_{36} = \left[\left(\frac{h_2}{2} + h_3 \right)^5 Q_{66}^T - \frac{h_2^5}{16} Q_{66}^T + \frac{h_2^5}{16} Q_{66}^C + \left(\frac{h_2}{2} + h_1 \right)^5 Q_{66}^T \right];$

$C_{39} = \left[\left(\frac{h_2}{2} + h_3 \right)^7 Q_{66}^T - \frac{h_2^7}{64} Q_{66}^T + \frac{h_2^7}{64} Q_{66}^C + \left(\frac{h_2}{2} + h_1 \right)^7 Q_{66}^T \right];$

$D_{11} = (h_1 Q_{55}^T + h_2 Q_{55}^C + h_3 Q_{55}^T); \quad D_{12} = \left[\left(\frac{h_2}{2} + h_3 \right)^3 Q_{55}^T - \frac{h_2^3}{4} Q_{55}^T + \frac{h_2^3}{4} Q_{55}^C + \left(\frac{h_2}{2} + h_1 \right)^3 Q_{55}^T \right];$

$D_{21} = (h_1 Q_{44}^T + h_2 Q_{44}^C + h_3 Q_{44}^T); \quad D_{22} = \left[\left(\frac{h_2}{2} + h_3 \right)^3 Q_{44}^T - \frac{h_2^3}{4} Q_{44}^T + \frac{h_2^3}{4} Q_{44}^C + \left(\frac{h_2}{2} + h_1 \right)^3 Q_{44}^T \right];$

$E_{11} = \left[K Q_{55}^T \left(\frac{h_2}{2} + h_3 \right)^3 - Q_{55}^T \frac{h_2^3}{4} + Q_{55}^T \left(\frac{h_2}{2} + h_1 \right)^3 + Q_{55}^C \frac{h_2^3}{4} \right];$

$E_{12} = \left[Q_{55}^T \left(\frac{h_2}{2} + h_3 \right)^5 - Q_{55}^T \frac{h_2^5}{16} + Q_{55}^T \left(\frac{h_2}{2} + h_1 \right)^5 + Q_{55}^C \frac{h_2^5}{16} \right];$

$E_{21} = \left[Q_{44}^T \left(\frac{h_2}{2} + h_3 \right)^3 - Q_{44}^T \frac{h_2^3}{4} + Q_{44}^T \left(\frac{h_2}{2} + h_1 \right)^3 + Q_{44}^C \frac{h_2^3}{4} \right];$

$E_{22} = \left[Q_{44}^T \left(\frac{h_2}{2} + h_3 \right)^5 - Q_{44}^T \frac{h_2^5}{16} + Q_{44}^T \left(\frac{h_2}{2} + h_1 \right)^5 + Q_{44}^C \frac{h_2^5}{16} \right];$

Appendix B

$\Delta = (A_{11} A_{22} - A_{12} A_{21}) \quad A_{11}^* = (A_{12} A_{23} - A_{22} A_{13}) / \Delta; \quad A_{12}^* = (A_{12} A_{24} - A_{22} A_{14}) / \Delta;$

$A_{13}^* = (A_{12} A_{26} - A_{22} A_{15}) / \Delta; \quad A_{14}^* = (A_{12} A_{26} - A_{22} A_{16}) / \Delta; \quad A_{14}^* = (A_{12} A_{26} - A_{22} A_{16}) / \Delta;$

$A_{15}^* = A_{22} / \Delta; A_{16}^* = -A_{12} / \Delta; \quad A_{21}^* = (A_{21} A_{13} - A_{11} A_{23}) / \Delta; \quad A_{22}^* = (A_{21} A_{14} - A_{11} A_{24}) / \Delta;$

$A_{23}^* = (A_{21} A_{15} - A_{11} A_{25}) / \Delta; \quad A_{24}^* = (A_{21} A_{16} - A_{11} A_{26}) / \Delta; \quad A_{25}^* = A_{11} / \Delta; \quad A_{26}^* = -A_{21} / \Delta;$

$A_{33}^* = \frac{1}{A_{33}}; \quad A_{36}^* = -\frac{A_{36}}{A_{33}}; \quad A_{39}^* = -\frac{A_{39}}{A_{33}}$

Appendix C

$U_{11} = (Z_1 - 3c_1 T_1); \quad U_{13} = c_1 Y_{11}; \quad U_{14} = (2c_1 Y_{36} + c_1 Y_{11}); \quad U_{12} = (Z_2 - 3c_1 T_2); \quad U_{15} = (c_1 Y_{12} + 2c_1 Y_{36});$

$U_{16} = c_1 Y_{12}; \quad U_{17} = c_1 Y_{13}; \quad U_{18} = (c_1 Y_{14} + 2c_1 Y_{39} + c_1 Y_{13}); \quad U_{19} = c_1 Y_{14}; \quad U_{110} = c_1 Y_{16};$

$U_{111} = (c_1 Y_{16} + 2c_1 Y_{33} + c_1 Y_{15}); \quad U_{112} = c_1 Y_{15};$

$U_{21} = (3c_1 T_1 - Z_1); \quad U_{22} = (X_{11} - c_1 Y_{11}); \quad U_{24} = (X_{12} - c_1 Y_{12} + X_{36} - c_1 Y_{36}); \quad U_{25} = (X_{13} - c_1 Y_{13});$

$U_{26} = (X_{14} - c_1 Y_{14} + X_{39} - c_1 Y_{39}); \quad U_{27} = (X_{15} + X_{33} - c_1 Y_{15} - c_1 Y_{33}); \quad U_{28} = (X_{16} - c_1 Y_{16});$

$U_{31} = (X_{21} - c_1 Y_{36} + X_{36} - c_1 Y_{11}); \quad U_{32} = (3c_1 T_2 - Z_2); \quad U_{33} = (X_{36} - c_1 Y_{36}); \quad U_{34} = (X_{22} - c_1 Y_{12});$

$U_{35} = (X_{23} + X_{39} - c_1 Y_{39} - c_1 Y_{13}); \quad U_{36} = (X_{24} - c_1 Y_{14}); \quad U_{37} = (X_{25} - c_1 Y_{15});$

$U_{38} = (X_{26} + X_{33} - c_1 Y_{33} - c_1 Y_{16});$

$X_{11} = (B_{11}A_{11}^* + B_{12}A_{21}^* + B_{13} - c_1 B_{11}A_{13}^* - c_1 B_{12}A_{23}^* - B_{15}c_1);$

$X_{12} = (B_{12}A_{22}^* + B_{14} + B_{11}A_{12}^* - c_1 B_{11}A_{14}^* - c_1 B_{12}A_{24}^* - B_{16}c_1);$ $X_{13} = (-c_1 B_{11}A_{13}^* - c_1 B_{12}A_{23}^* - B_{15}c_1);$

$X_{14} = (-c_1 B_{11}A_{14}^* - c_1 B_{12}A_{24}^* - B_{16}c_1);$ $X_{15} = B_{11}A_{15}^* + B_{12}A_{26}^*;$ $X_{16} = B_{11}A_{16}^* + B_{12}A_{25}^*$

$X_{21} = (B_{21}A_{11}^* + B_{22}A_{21}^* + B_{23} - c_1 B_{21}A_{13}^* - c_1 B_{22}A_{23}^* - B_{25}c_1);$

$X_{22} = (B_{21}A_{12}^* + B_{22}A_{22}^* + B_{24} - c_1 B_{21}A_{14}^* - c_1 B_{22}A_{24}^* - B_{26}c_1);$

$X_{23} = (-c_1 B_{21}A_{13}^* - c_1 B_{22}A_{23}^* - B_{25}c_1);$

$X_{24} = (-c_1 B_{21}A_{14}^* - c_1 B_{22}A_{24}^* - B_{26}c_1);$ $X_{25} = (B_{21}A_{15}^* + B_{22}A_{26}^*);$ $X_{26} = (B_{21}A_{16}^* + B_{22}A_{25}^*);$

$X_{33} = -B_{33}A_{33}^*;$ $X_{36} = (B_{33}A_{36}^* + B_{36} - c_1 B_{33}A_{39}^* - B_{39}c_1);$ $X_{39} = 2(-c_1 B_{33}A_{39}^* - B_{39}c_1);$

$Y_{11} = (C_{11}A_{11}^* + C_{12}A_{21}^* + C_{13} - c_1 C_{11}A_{13}^* - c_1 C_{12}A_{23}^* - C_{15}c_1);$

$Y_{12} = (C_{11}A_{12}^* + C_{12}A_{22}^* + C_{14} - c_1 C_{11}A_{14}^* - c_1 C_{12}A_{24}^* - C_{16}c_1);$ $Y_{13} = (-c_1 C_{11}A_{13}^* - c_1 C_{12}A_{23}^* - C_{15}c_1);$

$Y_{14} = (-c_1 C_{11}A_{14}^* - c_1 C_{12}A_{24}^* - C_{16}c_1);$ $Y_{15} = (C_{11}A_{15}^* + C_{12}A_{26}^*);$

$Y_{16} = (C_{11}A_{16}^* + C_{12}A_{25}^*);$ $Y_{21} = (C_{21}A_{11}^* + C_{22}A_{21}^* + C_{23} - c_1 C_{21}A_{13}^* - c_1 C_{22}A_{23}^* - C_{25}c_1);$

$Y_{22} = (C_{21}A_{12}^* + C_{22}A_{22}^* + C_{24} - c_1 C_{21}A_{14}^* - c_1 C_{22}A_{24}^* - C_{26}c_1);$ $Y_{23} = (-c_1 C_{21}A_{13}^* - c_1 C_{22}A_{23}^* - C_{25}c_1);$

$Y_{24} = (-c_1 C_{21}A_{14}^* - c_1 C_{22}A_{24}^* - C_{26}c_1);$ $Y_{25} = (C_{21}A_{15}^* + C_{22}A_{26}^*);$ $Y_{26} = (C_{21}A_{16}^* + C_{22}A_{25}^*);$

$Y_{33} = (-C_{33}A_{33}^*);$ $Y_{36} = (C_{33}A_{36}^* + C_{36} - c_1 C_{33}A_{39}^* - C_{39}c_1);$ $Y_{39} = 2(-c_1 C_{33}A_{39}^* - C_{39}c_1);$

$Z_1 = (D_{11} - D_{12}3c_1);$ $Z_2 = (D_{21} - D_{22}3c_1);$ $T_1 = (E_{11} - 3c_1 E_{12});$ $T_2 = (E_{21} - 3c_1 E_{22})$

Appendix D

$J_{11} = (h_{11} + h_{141});$ $J_{12} = (h_{12} + h_{142});$ $J_{13} = h_{143};$ $J_{14} = \left(h_{151}\frac{64}{9\pi^2} + h_{152}\frac{16}{9\pi^2}\right);$

$J_{15} = \left(h_{153}\frac{64}{9\pi^2} + h_{154}\frac{16}{9\pi^2}\right);$ $J_{16} = (h_{13} + h_{157});$ $J_{17} = \left(h_{155}\frac{64}{9\pi^2} + h_{156}\frac{16}{9\pi^2}\right);$ $J_{18} = \frac{-16}{3\pi^2}(h_{144} + h_{145});$

$J_{19} = \frac{-1}{2}(h_{158} + h_{159})$

$J_{21} = (h_{21} + h_{241});$ $J_{22} = (h_{22} + h_{242});$ $J_{23} = h_{243};$ $J_{24} = h_{23};$ $J_{25} = h_{244}\frac{32}{3\pi^2};$ $J_{31} = (h_{31} + h_{341});$

$J_{32} = (h_{32} + h_{342});$ $J_{33} = h_{343};$ $J_{34} = h_{33};$ $J_{35} = h_{344}\frac{32}{3\pi^2};$

where

$h_{11} = (-U_{11}\alpha + U_{13}\alpha^3 + U_{14}\alpha\beta^2);$ $h_{12} = (-U_{12}\beta + U_{15}\alpha^2\beta + U_{16}\beta^3);$

$h_{13} = (-U_{11}\alpha^2 - U_{12}\beta^2 + U_{17}\alpha^4 + U_{18}\alpha^2\beta^2 + U_{19}\beta^4 - k_1 - k_2\alpha^2 - k_2\beta^2);$

$h_{141} = H_3\left(U_{110}\alpha^4 + U_{111}\alpha^2\beta^2 + U_{112}\beta^4 - \alpha^2\frac{1}{R_y} - \beta^2\frac{1}{R_x}\right);$

$h_{142} = H_4\left(U_{110}\alpha^4 + U_{111}\alpha^2\beta^2 + U_{112}\beta^4 - \alpha^2\frac{1}{R_y} - \beta^2\frac{1}{R_x}\right);$

$h_{143} = H_5(U_{110}\alpha^4 + U_{111}\alpha^2\beta^2 + U_{112}\beta^4 - \alpha^2\frac{1}{R_y} - \beta^2\frac{1}{R_x});$ $h_{144} = H_1\left(U_{110}16\alpha^4 - 4\alpha^2\frac{1}{R_y}\right);$

$h_{145} = H_2\left(U_{112}16\beta^4 - 4\beta^2\frac{1}{R_x}\right);$

$h_{151} = 2\alpha^2\beta^2 H_3;$ $h_{152} = -2\alpha^2\beta^2 H_3;$ $h_{153} = 2\alpha^2\beta^2 H_4;$ $h_{154} = -2\alpha^2\beta^2 H_4;$ $h_{155} = 2\alpha^2\beta^2 H_5;$

$h_{156} = -2\alpha^2\beta^2 H_5;$ $h_{157} = -\alpha^2 N_{x0} - \beta^2 N_{y0};$ $h_{158} = 4\alpha^2\beta^2 H_1;$ $h_{159} = 4\alpha^2\beta^2 H_2;$

$h_{21} = (U_{21} - U_{22}\alpha^2 - U_{23}\beta^2);$ $h_{22} = (-U_{24}\alpha\beta);$ $h_{23} = (U_{21}\alpha - U_{25}\alpha^3 - U_{26}\alpha\beta^2);$

$h_{241} = H_3(-\alpha\beta^2 U_{27} - \alpha^3 U_{28});$ $h_{242} = H_4(-\alpha\beta^2 U_{27} - \alpha^3 U_{28});$ $h_{243} = H_5(-\alpha\beta^2 U_{27} - \alpha^3 U_{28});$ $h_{244} = 8\alpha^3 U_{28} H_1;$

$h_{31} = (-\alpha\beta U_{31});$ $h_{32} = (U_{32} - U_{33}\alpha^2 - U_{34}\beta^2);$ $h_{33} = (U_{32}\beta - U_{35}\alpha^2\beta - U_{36}\beta^3);$

$h_{341} = H_3(-\beta^3 U_{37} - \alpha^2\beta U_{38});$ $h_{342} = H_4(-\beta^3 U_{37} - \alpha^2\beta U_{38});$ $h_{343} = H_5(-\beta^3 U_{37} - \alpha^2\beta U_{38});$

$h_{344} = 8\beta^3 U_{37} H_2;$

References

[1] Gabriele Imbalzano, Phuong T, Tuan ND, Lee Peter VS. Three-dimensional modelling of auxetic sandwich panels for localised impact resistance. J Sandwich Struct Mater 2015;19(3):291–316.

[2] Whitty JPM, Alderson A, Myler P, Kandola B. Towards the design of sandwich panel composites with enhanced mechanical and thermal properties by variation of the in-plane Poisson's ratios. Compos A 2003;34:525–34.

[3] Ruzzene Massimo, Mazzarella Luca, Tsopelas Panagiotis, Scarpa Fabrizio. Wave propagation in sandwich plates with periodic auxetic core. J Intell Mater Syst Struct 2002;13(9):587–97.

[4] Qing-Tian D, Zhi-Chun Y. Wave propagation in sandwich panel with auxetic core. J Solid Mech 2010;2(4):393–402.

[5] Qiao JX, Chen CQ. Impact resistance of uniform and functionally graded auxetic double arrowhead honeycombs. Int J Impact Eng 2015;83:47–58.

[6] Miller W, Ren Z, Smith CW, Evans KE. A negative Poisson's ratio carbon fibre composite using a negative Poisson's ratio yarn reinforcement. Compos Sci Technol 2012;72(7):761–6.

[7] Zhang G, Ghita OR, Evans KE. Dynamic thermo-mechanical and impact properties of helical auxetic yarns. Compos Part B Eng 2016;99:494–505.

[8] Strek T, Jopek H, Nienartowicz M. Dynamic response of sandwich panels with auxetic cores. Phys Status Solidi Basic Res 2015;252(7):1540–50.

[9] Ghaznavi A, Shariyat M. Non-linear layerwise dynamic response analysis of sandwich plates with soft auxetic cores and embedded SMA wires experiencing cyclic loadings. Compos Struct 2017;171:185–97.

[10] Jin Xiaochao, Wang Zhihua, Ning Jianguo, Xiao Gesheng, Liu Erqiang, Shu Xuefeng. Dynamic response of sandwich structures with graded auxetic honeycomb cores under blast loading. Compos B Eng 2016;106:206–17.

[11] Sofiyev AH, Hui D, Huseynov SE, Salamci MU, Yuan GQ. Stability and vibration of sandwich cylindrical shells containing a functionally graded material core with transverse shear stresses and rotary inertia effects. Proc I Mech E, Part C: J Mech

Eng Sci 2016;230(14):2376–89.

[12] Li X, Zhang PW, Wang ZH, Wu GY, Zhao LM. Dynamic behavior of aluminum honeycomb sandwich panels under air blast: experiment and numerical analysis. Compos Struct 2014;108:1001–8.

[13] Duc ND, Cong PH. Nonlinear dynamic response and vibration of sandwich composite plates with negative Poisson's ratio in auxetic honeycombs. J Sandwich Struct Mater 2016http://journals.sagepub.com/doi/pdf/10.1177/1099636216674729.

[14] Duc ND, Kim Seung-Eock, Tuan ND, Phuong T, Khoa ND. New approach to study nonlinear dynamic response and vibration of sandwich composite cylindrical panels with auxetic honeycomb core layer. J Aerosp Sci Technol 2017;70:396–404.

[15] Duc ND, Kim Seung-Eock, Cong PH, Anh NT, Khoa ND. Dynamic response and vibration of composite double curved shallow shells with negative Poisson's ratio in auxetic honeycombs core layer on elastic foundations subjected to blast and damping loads. Int J Mech Sci 2017;113:504–12.

[16] Lam Nelson, Mendis Priyan, Tuan ND. Response spectrum solutions for blast loading. Electron J Struct Eng 2004;4:28–44.

[17] Yong Lu, Wang Zhongqi, Chong Karen. A comparative study of buried structure in soil subjected to blast load using 2D and 3D numerical simulations. Soil Dyn Earthquake Eng 2005;25(4):275–88.

[18] T-uacute, rkmen Halit S, Mecitoglu Zahit. Nonlinear structural response of laminated composite plates subjected to blast loading. AIAA J 1999;37(12):1639–47.

[19] Duc ND, Tuan ND, Phuong T, Quan TQ. Nonlinear dynamic response and vibration of imperfect shear deformable functionally graded plates subjected to blast and thermal loads. Mech Adv Mater Struct 2017;24(4):318–29.

[20] Imbalzano Gabriele, Linforth Steven, Tuan ND, Peter VS, Phuong T. Blast resistance of auxetic and honeycomb sandwich panels: Comparisons and parametric designs. Compos Struct 2017. http://dx.doi.org/10.1016/j.compstruct.2017.03.018.

[21] Imbalzano Gabriele, Phuong T, Tuan ND, Peter VS. A numerical study of auxetic composite panels under blast loadings. Compos Struct 2016;135:339–52.

[22] Duc ND. Nonlinear static and dynamic stability of functionally graded plates and shells. Hanoi: Vietnam National University Press; 2014.

[23] Cong PH, Anh VM, Duc ND. Nonlinear dynamic response of eccentrically stiffened FGM plate using Reddy's TSDT in thermal environment. J Thermal Stresses 2017;40(6):704–32.

[24] Khoa ND, Thiem HT, Duc ND. Nonlinear buckling and postbuckling of imperfect piezoelectric S-FGM circular cylindrical shells with metal-ceramic-metal layers in thermal environment using Reddy's third-order shear deformation shell theory. J Mech Adv Mater Struct 2017. http://dx.doi.org/10.1080/15376494.2017.1341583.

[25] Quan TQ, Duc ND. Nonlinear vibration and dynamic response of shear deformable imperfect functionally graded double curved shallow shells resting on elastic foundations in thermal environments. J Therm Stresses 2016;39(4):437–59.

[26] Kolahchi Reza, Zareib Mohammad Sharif, Hajmohammad Mohammad Hadi, Oskoueic Alireza Naddaf. Visco-nonlocal-refined Zigzag theories for dynamic buckling of laminated nanoplates using differential cubature-Bolotin methods. Thin-Walled Struct 2017;113:162–9.

[27] Shokravi Maryam. Dynamic pull-in and pull-out analysis of viscoelastic nanoplates under electrostatic and Casimir forces via sinusoidal shear deformation theory. Microelectron Reliab 2017;71:17–28.

[28] Kolahchi Reza, Safari Morteza, Esmailpour Masoud. Dynamic stability analysis of temperature-dependent functionally graded CNT-reinforced visco-plates resting on orthotropic elastomeric medium. Compos Struct 2016;150(15):255–65.

[29] Madani Hamid, Hosseini Hadi, Shokravi Maryam. Differential cubature method for vibration analysis of embedded FG-CNT-reinforced piezoelectric cylindrical shells subjected to uniform and non-uniform temperature distributions. Steel Compos Struct 2016;22(4):889–913.

[30] Kolahchi Reza, Zarei Mohammad Sharif, Hajmohammad Mohammad Hadi, Nouri Ali. Wave propagation of embedded viscoelastic FG-CNT-reinforced sandwich plates integrated with sensor and actuator based on refined zigzag theory. Int J Mech Sci 2017;130:534–45.

[31] Reddy JN. Mechanics of laminated composite plates and shells; theory and analysis. Boca Raton: CRC Press; 2004.